ISBN: 978-3-95450-227-1 ISSN: 2673-5490 doi:10.18429/JACoW-IPAC2022-WEPOPT037

DYNAMIC APERTURE EVALUATION FOR EIC HADRON STORAGE RING WITH CRAB CAVITIES AND IR NONLINEAR MAGNETIC FIELD ERRORS*

Y. Luo†, X. Gu, J. S. Berg, W. Fischer, H. Lovelace III, C. Montag,
S. Peggs, V. Ptitsyn, H. Witte, D. Xu, Brookhaven National Laboratory, Upton, NY, USA
Y. Hao, Facility for Rare Isotope Beams, Michigan State University, East Lansing, MI, USA
J. Qiang, Lawrence Berkeley National Laboratory, Berkeley, CA, USA
V. Morozov, T. Satogata, Thomas Jefferson National Accelerator Facility, Newport News, VI, USA

Abstract

The Electron-Ion Collider (EIC) presently under construction at Brookhaven National Laboratory will collide polarized high energy electron beams with hadron beams with luminosities up to $1 \times 10^{34}\text{cm}^{-2}\text{s}^{-1}$ in the center mass energy range of 20-140 GeV. In this article, we evaluate the dynamic aperture for the Hadron Storage Ring (HSR) with symplectic element-by-element tracking. Crab cavities, nonlinear magnetic field errors, and weak-strong beam-beam interaction are included. We compared the dynamic aperture with crossing-angle collision to head-on collision and found the reason for the dynamic aperture reduction. We also studied the field error tolerances for IR magnets and for some particular magnets.

INTRODUCTION

The Electron-Ion Collider (EIC) presently under construction at Brookhaven National Laboratory will collide polarized high energy electron beams with hadron beams with luminosities up to $1 \times 10^{34}\text{cm}^{-2}\text{s}^{-1}$ in the center mass energy range of 20-140 GeV [1]. We focus on the collision mode involving 275 GeV protons and 10 GeV electrons since at this collision mode both protons and electrons reach their highest beam-beam parameters in EIC. Table 1 lists the beam-beam related design parameters for this study. In this article, we will evaluate the dynamic aperture calculation for the 275 GeV protons in the Hadron Storage Ring (HSR).

The HSR of EIC will re-use the existing RHIC arcs. Based on RHIC operational experience [2], simulated dynamic aperture in 10^6 turns with beam-beam interaction and IR nonlinear field errors should be larger than 5 σ with 3 $(dp/p_0)_{rms}$ to guarantee an acceptable beam lifetime at physics store. The beam-beam parameter for the proton beam in HSR is 0.012 which is comparable to RHIC, therefore we require the minimum dynamic aperture for HSR should be larger than 5 σ too.

SIMULATION SETUP

There are a few new features for HSR than RHIC [3]. First, EIC adopts a full crossing angle of 25 mrad at IP. To compensate the geometric luminosity loss due to the crossing angle, crab cavities are used to restore head-on collision. For EIC, local crabbing scheme is adopted. Ideally, crab cavities are placed on both sides of IP with a horizontal phase advance $\pi/2$ to IP.

To match the revolution frequency of Electron Storage Ring (ESR), HSR needs to be able to adjust its path length at various beam energies, which is achieved with radial shift orbit in arcs. The radial shift orbit is created with a field deviation from the nominal design value by $\Delta B/B_0$ to arc bending dipoles. Therefore, the on-momentum particle does not always have zero longitudinal coordinate $z = -c(t - t_0)$ in tracking code, where t_0 is the time flight on the reference orbit.

Based on the RHIC operational experience, IR magnetic field errors play an important role in dynamic aperture reduction. At the design phase of EIC, we will artificially assign magnetic field errors to all IR dipoles and quadruples within 160 m from IP to evaluate their impacts on the dynamic aperture of HSR.

Magnet field errors are defined as

$$(B_y L) + i(B_x L) = B(R_{ref}) L \left[10^{-4} \sum_{n=0}^{N_{max}} (b_n + i a_n) \frac{(x+iy)^n}{R_{ref}^n} \right]. \quad (1)$$

Here L is the magnet length, R_{ref} is the reference radius where the magnetic field is measured, $B(R_{ref})$ is the main field at R_{ref}, b_n and a_n are the coefficients for normal and skew magnetic components.

Both systematic and random field errors can be assigned in the simulation. Here we focus on random field errors. In our study, we normally excluded the dipole and quadrupole

Table 1: Beam-beam Related Machine and Beam Parameters for Collision Between 275 GeV Protons and 10 GeV Electrons

quantity	unit	proton	electron
Beam energy	GeV	275	10
Bunch intensity	10^{11}	0.668	1.72
(β_x^*, β_y^*) at IP	cm	(80, 7.2)	(55, 5.6)
Beam sizes at IP	μm	(95, 8.5)	
Bunch length	cm	6	0.7
Energy spread	10^{-4}	6.8	5.8
Transverse tunes		(0.228, 0.210)	(0.08, 0.06)
Longitudinal tune		0.01	0.069

* Work supported by Brookhaven Science Associates, LLC under Contract No. DE-SC0012704 with the U.S. Department of Energy.
† yluo@bnl.gov

ISBN: 978-3-95450-227-1 ISSN: 2673-5490 doi:10.18429/JACoW-IPAC2022-WEPOPT037

components since we are able to correct orbit and tunes during operation.

Dynamic aperture is calculated with a 6-d symplectic particle tracking code SimTrack [4]. For each study condition, test particles are launched in the first quadrant of phase space $(x/\sigma_x, y/\sigma_y)$ in 5 equal distance phase angles. Test particles are tracked up to 1 million turns. We focus on the minimum dynamic aperture among those 5 phase angles. To determine IR field error tolerances, 10 sets of random field errors are currently used.

SIMULATION RESULTS

DA Drop with Crossing Angle Collision

First we calculate the dynamic apertures with IR nonlinear field errors with head-on and crossing angle collisions. Figure 1 shows the dynamic apertures for both cases as function of IR field errors. The horizontal axis is the units of b_n and a_n, the vertical axis is the minimum dynamic aperture among all phase angles of 10 seeds. For this calculation, particle's relative momentum deviation $dp/p_0 = 20 \times 10^{-4}$, which is about $3(dp/p_0)_{rms}$.

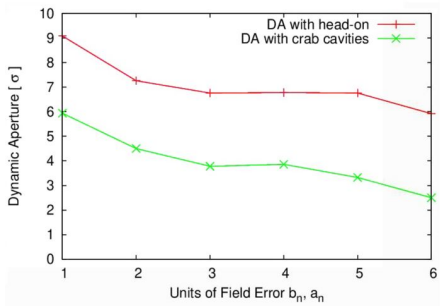

Figure 1: Dynamic aperture with IR field errors for head-on collision and crossing angle collision.

From the plot, the dynamic apertures for both head-on and crossing angle collisions decrease with increase in IR magnetic field errors. For 1 unit of magnetic field errors, the dynamic aperture with crossing angle collision is about 6σ, which seems sufficient for proton beam's lifetime according to RHIC's operational experience.

From the plot, we notice that there is about 3σ drop in dynamic aperture from head-on collision to crossing angle collision. In principle, with crossing angle collision and crab cavities, head-on collision is restored and their dynamic aperture should be the same or close. In the following, we will look for the reasons for this dynamic aperture drop.

Figure 2 compares the dynamic apertures for head-on and crossing angle collisions without IR nonlinear field errors. The horizontal axis is the particle's relative momentum deviation from zero up to 20×10^{-4}. From the plot, there are not much difference in the dynamic apertures between those two cases for the shown dp/p_0 range.

Figure 3 compares the dynamic apertures for head-on and crossing angle collisions with IR nonlinear field errors. The IR field errors is 1 unit for all b_n and a_n. From the

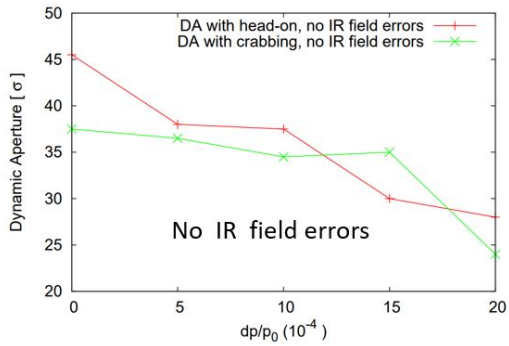

Figure 2: Dynamic aperture as function of dp/p_0 without IR field errors.

plot, the dynamic aperture for head-on is higher than that with crossing angle collision. When the relative momentum deviation increases, especially from 10×10^{-4} to 20×10^{-4}, the gap in the dynamic apertures between those two cases gets bigger. With $dp/p_0 = 20 \times 10^{-4}$, the difference is 3σ.

From above comparisons, we learned that the dynamic aperture reduction from head-on collision to crossing angle collision is related to IR nonlinear field errors. As we know, with local crabbing scheme, particles with non-zero longitudinal offset z will have an additional horizontal offset $\Delta x = \zeta \times z$, where $\zeta = dx/dz$ is the crab dispersion.

For example, Figure 4 shows a test particle's horizontal trajectories across the interaction region with different sets of initial z and dp/p_0. Test particles are launched from one side crab cavities toward other side. From the plot, particles with non-zero z will have a sizable horizontal orbit in IR.

Particles with non-zero z will sample larger IR field errors. Considering synchrotron motion, it is true too for particles with non-zero dp/p_0. The larger the momentum deviation is, the greater IR magnetic field errors they will feel. To minimize the dynamic aperture drop with crossing angle collision, we should reduce IR nonlinear magnetic field errors.

Updated Reference Radius

Based on Eq. (1), IR magnetic field error coefficients b_n and a_n depend on the reference radius R_{ref}. In the previous

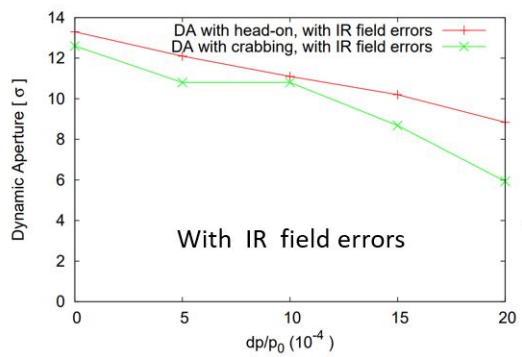

Figure 3: Dynamic aperture as function of dp/p_0 with IR field errors.

ISBN: 978-3-95450-227-1 ISSN: 2673-5490 doi:10.18429/JACoW-IPAC2022-WEPOPT037

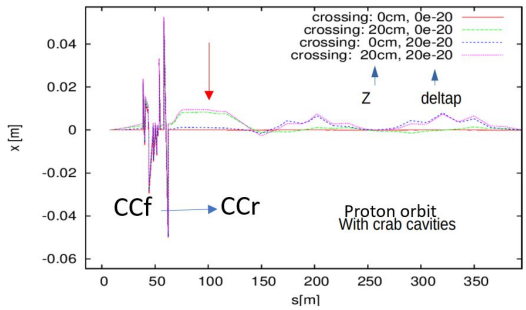

Figure 4: Horizontal trajectories across IR with different combinations of z and dp/p_0.

dynamic aperture studies for the HSR, we set the reference radius to be 60 mm for all IR dipoles and 40 mm for all IR quadrupoles. With the progresses in the HSR magnet design, we have better knowledge of reference radius for IR magnets. Table 2 shows the updated reference radius that should be used from now on. In the table, near side or farther side means the two ends of magnets facing IP or away from IP.

Different Random Number Generation

In the previous dynamic aperture calculation, we assigned IR field errors with an uniform random number generator. For example, for 1 unit of b_n or a_n, their values from random number generator can vary from -1 to 1. As noted above, currently we use 10 seeds of random IR field errors for each simulation condition.

We compared the dynamics apertures with different random number generators. For example, for a Gaussian random number generator, with 1 unit of field errors of b_n and a_n, the actual values of errors can be more than 1 unit but the statistical standard deviation will stay 1 unit for many seeds.

Table 3 compares the dynamic apertures with uniform and Gaussian distribution generators for IR nonlinear magnetic field errors. From Table 3, the dynamic aperture is normally larger with an uniform random number generator than with a Gaussian generator. The reason is that the random filed errors with Gaussian distribution can go higher than the uniform distribution. For the EIC, considering a small number of IR magnets, we prefer uniform distribution of IR field errors in simulation.

Table 2: Updated Reference Radius for IR Magnets

Magnet	R1 (mm)	R2 (mm)	R_{ref} (mm)
Name	near side	farther side	used in simualton
B0pF	IP	non-IP	60
B0ApF	43	43	43
Q1ApF	44	33.5	44
Q1BpF	55	32	55
Q2pF	73	73	73
B1pF	40	55	55
B1ApF	63	63	63
Q1ApR	26	26	26
Q1BpR	28	28	28
Q2pR	54	54	54

Field Tolerances for a Large Aperture Magnet

There are some large physical aperture magnets in the IR6 of HSR. Magnetic field errors may get big away from the center of beam pipe. We paid particular attention to a large aperture dipole B2PF, which is just in front of the crab cavities in the forward side of IR6. Its reference radius is 50 mm. In the dynamic aperture calculation, we set same units for all b_n and a_n from sextupole component to 11th pole. Table 4 shows the simulated dynamic aperture with B2PF's field errors. To have dynamic aperture not less than 6σ for the HSR lattice, B2PF's field errors b_n and a_n should be below 1 units.

SUMMARY

In this article, we presented the simulation setup and the main concerns for the dynamic aperture calculation for the HSR of EIC. We identified the reason for the dynamic aperture drop from head-on collision to crossing angle collision. To improve dynamic aperture with crossing angle collision, we should have a good control of magnetic field errors in the interaction region. We updated the reference radius for magnetic field errors and tested with different ways of random number generation. The tolerance of field errors for the large aperture dipole B2PF should be less than 1 unit.

Table 3: Dynamic Aperture Comparison with Uniform and Gaussian Random Number Generation

	Uniform Distr.			Gaussian Distr.		
unit	min	ave	rms	min	ave	rms
0.0	19.4	19.4	0	17.8	19.2	0.5
0.3	5.8	9.1	1.6	6.8	9.5	1.4
0.6	5.8	8.1	1.5	3.4	7.18	1.9
0.9	6.2	7.9	0.7	3.8	6.88	1.6
1.2	4.8	6.7	1.3	5.0	7.22	1.0
1.5	4.8	7.1	1.4	5.2	6.58	0.8
1.8	4.0	7.3	2.0	3.8	5.56	1.3
2.1	5.6	7.0	1.1	5.0	6.76	1.3
2.4	4.8	6.0	0.7	3.2	5.32	1.2
2.7	4.2	6.2	1.1	2.2	5.36	1.3

Table 4: Dynamic Aperture Versus B2PF's Magnetic Field Errors

Unit	DA-Min	DA-Max	DA-Ave	DA-RMS
1	5.0	7.6	6.2	0.8
2	2.2	5.4	3.9	0.8
3	2.6	4.2	3.6	0.5
4	1.8	3.4	2.5	0.5
5	1.4	2.8	1.8	0.4

ISBN: 978-3-95450-227-1 ISSN: 2673-5490 doi:10.18429/JACoW-IPAC2022-WEPOPT037

REFERENCES

[1] C. Montag *et al.*, "Design Status Update of the Electron-Ion Collider", in *Proc. IPAC'21*, Campinas, Brazil, May 2021, pp. 2585–2588. doi:10.18429/JACoW-IPAC2021-WEPAB005

[2] Y. Luo, W. Fischer and S. White, "Analysis and modeling of proton beam loss and emittance growth in the Relativistic Heavy Ion Collider", *Phys. Rev. Accel. Beams*, vol. 19, p. 021001, American Physical Society, Feb. 2016. doi:10.1103/PhysRevAccelBeams.19.021001

[3] Y. Luo *et al.*, "Dynamic Aperture Evaluation for the Hadron Storage Ring in the Electron-Ion Collider", in *Proc. IPAC'21*, Campinas, Brazil, May 2021, pp. 3812–3814. doi:10.18429/JACoW-IPAC2021-THPAB029

[4] Y. Luo, "SimTrack: A compact c++ code for particle orbit and spin tracking in accelerators", *Nucl. Instrum. Methods Phys. Res., Sect. A*, vol. 801, pp. 95-103, 2015. doi:10.1016/j.nima.2015.08.014